

## ASSESSMENT OF THE ACCURACY OF A VIRTUAL MULTI-CHANNEL TEMPERATURE MEASURING INSTRUMENT

Romuald Mańnicki<sup>1\*</sup>, Beata Pałczyńska<sup>2</sup>

<sup>1</sup> Gdynia Maritime University, 81-87 Morska St., 81-225 Gdynia, Poland, Faculty of Electrical Engineering, Department of Marine Electrical Power Engineering, ORCID 0000-0002-4224-528X, e-mail: r.masnicki@we.umg.edu.pl

<sup>2</sup> Gdańsk University of Technology, 11/12 Gabriela Narutowicza St., 80-233 Gdańsk, Poland, Faculty of Electrical and Control Engineering, Department of Metrology and Information Systems, ORCID 0000-0002-2404-6500, e-mail: beata.palczynska@pg.edu.pl

\* Corresponding author

**Abstract:** The multi-channel temperature measurement system developed works with NTC thermistors. The article presents the results of theoretical and empirical evaluation of accuracy obtained in measurement channels. The basis for the theoretical assessment is the mathematical model for each of the measurement channels and the characteristics of the system elements included in the circuits of the measurement channel. Two different methods were used to theoretically estimate the accuracy: the Gauss Formula and the Monte Carlo method. The empirical assessment of accuracy is supported by measurement data collected during the calibration procedures for the device developed and the results of verification measurements performed on a working device. The exemplary results presented of the accuracy assessment, obtained in the selected channel, are representative of the properties of all other measurement channels. The results of both methods of assessing accuracy in measurement channels are very similar, which confirms the assumptions regarding the implementation of the instrument developed and its good metrological properties.

**Keywords:** accuracy evaluation, uncertainty, temperature measurement, multi-channel instrument, NTC thermistor.

### 1. INTRODUCTION

As a part of the research conducted at the Department of Marine Electrical Power Engineering of the Gdynia Maritime University, a multi-channel virtual instrument was developed [Masnicki and Swisulski 2023]. Although the device was developed primarily for measuring the temperature distribution in a laboratory model of an underground power line with casing pipes [Masnicki, Mindykowski and Palczynska 2022], this device can be implemented in many other applications.

Basic operations in all its measurement channels are performed in software on digital data. The hardware configuration of the instrument is shown in Figure 1. The instrument is based on NI PXI (National Instruments PCI eXtensions for Instrumentation) Measurement Platform 1 with user interface (screen, keyboard and mouse) and NI Terminal Block 2 cooperating with a set of NTC (Negative Temperature Coefficient) thermistors. The temperature information is obtained from the thermistors [NTC Thermistor 2017] and is further processed in the NI LabVIEW environment. A temperature calibrator 3 (T-704 Mors) was applied to set specific temperatures during the calibration of measurement channels and during the testing of their properties. The digital temperature meter 4 (DT-34 Termoprodukt) [Thermometer DT-34 2023] was used as a reference instrument to verify the temperature setting.

A single temperature sensing circuit uses an additional resistor  $R_i$  (Fig. 2) connected in a series with the NTC thermistor  $R_{Ti}$ , which forms a thermistor conditioning circuit as a voltage divider, whose output voltage is fed into the input of the NI DAQ (Data Acquisition) card installed in the NI PXI measurement platform. For all measurement channels, the additional resistors  $R_i$  are placed on the PCB (Printed Circuit Board) in the NI Terminal Block 2 (Fig. 1). NTC thermistors, located on the measured object, have cable connections to their conditioning circuits. The eleven input channels of the NI DAQ card (Fig. 2) are used for making the measurements in the studies mentioned in the Introduction. Channel 0 (ch\_0) is used to measure the voltage  $U_z$  supplied to the thermistor conditioning circuits, and another ten channels (ch\_1 - ch\_10) are used to measure the output voltages  $U_i$  from voltage dividers. Figure 2 shows the thermistor cables connected to the pins on the NI Terminal Block.



**Fig. 2.** Components of the developed multi-channel instrument: 1 – NI PXI measurement platform with NI DAQ card, 2 – NI Terminal Block, 3 - temperature calibrator, 4 – digital thermometer

Source: [Masnicki and Swisulski 2023].

NI PXI measurement platform 1 (Figure 1) consists of the NI PXIe-1082Q (National Instruments Chassis) housing [NI PXIe-1082 2023], which is equipped with the NI PXIe-8135 (Embedded Controller) [NI PXIe-1035 2023] and NI PXIe-6341 (DAQ card) [NI PXIe-6341 2023]. The NI SH68M-68F-EPM cable (68-pin male VHDCI to 68-pin female D-SUB connector) connects the NI Terminal Block 2 [NI SCB-68A 2023] to the DAQ card. The NI PXIe-1082Q is an 8-Slot chassis (with 4 hybrid slots, 2 PXIe Slots and 1 PXIe System Timing Slot). The NI PXIe-8135 is an embedded Quad-Core 2.3 GHz (Intel Core i7) controller for NI PXI Express systems. The NI PXIe-6341 DAQ card includes, among others, 16 analogue inputs (16-Bit, 500 kS/s), 2 analogue outputs, 24 digital I/O, and four 32-bit counter/timers for PWM. The DAQ input channels in developed system were configured in the NI Terminal Block to operate in the RSE (Referenced Single-Ended) mode.

In the case of instruments with software digital data processing, the key role in the measurement channels is played by software algorithms, which largely determine their properties and the quality of the measurement process. Virtual instrument means a fully functional measuring instrument (or system) in which basic functions performed in hardware in traditional measurement circuits, such as correction of processing characteristics or mathematical operations on signals, have been transferred to software and are digital data operations implemented in software procedures. This has an impact on the assessment of the accuracy of the measurements.

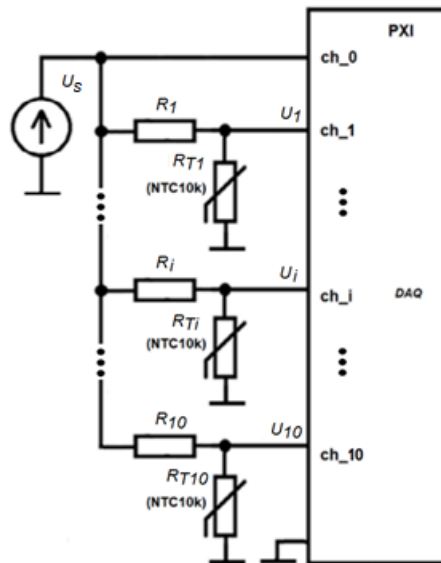


**Fig. 2.** Thermistor application circuits

Source: [Masnicki and Swisulski 2023].

The main goal set in the article is to assess the measurement accuracy of the developed channels for temperature measurement, both theoretically and on the basis of experimental verification measurements.

In the relevant literature, a certain proposal for analysing this issue is presented in [Liu, Pan and Cai 2012] for multi-point temperature measurement. The author [Samoilenko 2021] demonstrates how to choose the best evaluation of uncertainty from many variants of solutions depending on mathematical models of measurement. [Pawlowski, Szlachta and Otomański 2023] presents the results of research aimed at developing a method and a measuring stand for the experimental evaluation of uncertainty in a measuring system using data acquisition modules containing analogue-to-digital converters. Sarbu (2018) refers to evaluation of measurement uncertainty in calibration of thermoresistances.

In the paper presented, the theoretical evaluation was carried out using mathematical models describing the characteristics of the measurement channels, and the experimental evaluation was carried out by examining the properties of the temperature channels during reference temperature measurements.

The paper is organised as follows: Section 2 contains an analysis of the sources of measurement errors affecting measurement results and focuses on the formulation of a mathematical model of the measurement channel. Section 3 presents the theoretical and empirical evaluation of the accuracy of measurement results. This section presents the basic assumptions of the conducted analyses of the accuracy of



temperature measurements and the results obtained. In Section 4, the final conclusions are drawn.

## 2. MATHEMATICAL MODEL OF THE MEASUREMENT CHANNEL

The mathematical model of the measurement channel  $i$  in the system shown in Figure 2 takes into account the conversion of measured temperature  $T$  into resistance  $R_{Ti}$ , and then  $R_{Ti}$  into voltage  $U_i$ , the input voltage of the ADC. Finally the voltage  $U_i$  is converted in ADC into its digital representation.

NTC10k thermistors, hermetic miniature sensors with a resistance of 10 k $\Omega$  at a temperature of 25 °C, were used as temperature sensors in the measuring system developed. The manufacturer of the NTC10k thermistors under consideration declares in the datasheet [NTC Thermistor 2017] that the sensor  $R_T$  resistance at 25°C is 10 k $\Omega$   $\pm$ 1%, and its coefficient  $\beta$  is 3380 K  $\pm$ 1%. To describe the non-linear characteristics of the thermistors used in the research as the relationship between the resistance of the thermistor and the measured temperature, the commonly used equation (1) with the material constant  $\beta$  was considered [Steinhart and Hart 1968].

$$R_T = R_{T_0} \cdot e^{\beta \left( \frac{1}{T} - \frac{1}{T_0} \right)} \quad (1)$$

Where:

- $R_T$  [ $\Omega$ ] – sensor resistance at measured temperature  $T$  [K],
- $R_{T_0}$  [ $\Omega$ ] – sensor resistance at reference temperature  $T_0$  [K],
- $\beta$  [K] – material constant of the sensor.

The thermistor is included into the voltage divider circuit described in equation (2). It should be noted that the input resistance of each DAQ channel (here: 10 G $\Omega$ ) is much greater than the resistances used in the voltage divider, and its influence can be neglected in further analyses.

$$U_i = U_s \frac{R_{Ti}}{R_{Ti} + R_i} \quad (2)$$

Where:

- $U_s$  – supply voltage, common to voltage dividers in all channels,
- $U_i$  – the output voltage of the voltage divider in channel  $i$ ,
- $R_{Ti}$  – thermistor resistance in channel  $i$ ,
- $R_i$  – auxiliary resistor in voltage divider in channel  $i$ .

Hence, for any channel, the output voltage from the voltage divider can be written as:

$$U_i = U_s \frac{R_{T_0} \cdot e^{\beta \left( \frac{1}{T} - \frac{1}{T_0} \right)}}{R_{T_0} \cdot e^{\beta \left( \frac{1}{T} - \frac{1}{T_0} \right)} + R_i} \quad (3)$$

In order to determine the temperature value, in the software algorithms of the device, the mathematical operations described by the equation (4) obtained from the transformation (3) should be performed. Since in the LabVIEW environment, the digital data at the output of the DAQ card are available in units of input voltages, it is not necessary to take into account the processing characteristics of the ADC converter in the model.

$$T = \frac{\beta}{\ln \frac{U_i R_i}{(U_S - U_i) R_{T0}} + \frac{\beta}{T_0}} \quad (4)$$

The formula (4) is a mathematical representation of the measurement channel and will be the basis for a theoretical assessment of the accuracy of temperature measurement in individual channels.

### 3. THEORETICAL AND EMPIRICAL EVALUATION OF THE ACCURACY OF MEASUREMENT RESULTS

#### 3.1. Theoretical evaluation of uncertainty

The "Guide to the expression of uncertainty in measurement" (GUM) [JCGM 100 2008] describes two types of uncertainties, categorised as Type A and Type B, respectively. Type A uncertainty is based on the statistical analysis of a series of measurements. Type B uncertainty has been obtained by non-statistical procedures, i.e. based on the manufacturer's specifications. The final result of any measurement procedure should have an associated standard uncertainty obtained by combining Type A and Type B components.

The measurement uncertainty associated with the output quantity defined by a measurement model (4) can be evaluated using two different methods:

- Gauss Formula described in the GUM;
- The Monte Carlo method specified in GUM Supplements 1 [JCGM 101 2008] and 2 [JCGM 102 2011].

In this paper, the relevant calculations were made using a web-based software application produced by the National Institute of Standards and Technology (NIST) [NIST Uncertainty Machine 2023].

The six input quantities  $x_k$ :  $U_S$ ,  $U_i$ ,  $\beta$ ,  $R_i$ ,  $R_{T0}$ ,  $T_0$  of (4) are modelled as random variables with known probability distributions. The parameters of a distribution (a mean value and a standard deviation) are used to characterise their standard uncertainties of Type A  $u_A(x_k)$ .

In order to evaluate the Type B uncertainty, the AI (Analog Input) Absolute Accuracy of DAQ card  $\Delta_{DAQ}$  [NI PXIE-6341 2023] is considered. Engineering practice and theoretical considerations suggest that the distribution of the error

parameters can usually be similar to uniform distribution. Therefore, the relevant standard uncertainty of type B is:

$$u_B(x_k) = \frac{\Delta_{DAQ}}{\sqrt{3}} \quad (5)$$

According to the PXIe-6341 Specification, full scale AI Absolute Accuracy, at 10 V, is equal to 2.19  $\mu$ V. In this case, the Type B uncertainty is 1.26  $\mu$ V. This uncertainty should be considered when determining the uncertainty of all quantities whose values are calculated based on voltage measurements. This applies to individual quantities used to determine the temperature value (4).

Taking both types of uncertainty into account, the standard uncertainty is given by the following equation:

$$u(x_k) = \sqrt{u_A^2(x_k) + u_B^2(x_k)} \quad (6)$$

By applying the rule of propagation uncertainties to measurement model (4), the combined measurement uncertainty can be expressed by:

$$u_c(T(x_k)) = \sqrt{\sum_{k=1}^K \left( \frac{\partial T(x_k)}{\partial x_k} \right)^2 u^2(x_k) + 2 \sum_{k=1}^{K-1} \sum_{i=k+1}^K \frac{\partial T(x_k)}{\partial x_k} \frac{\partial T(x_k)}{\partial x_i} u(x_k, x_i)} \quad (7)$$

Where:

$$\frac{\partial T(x_k)}{\partial x_k} \quad \text{– a sensitivity coefficient,}$$

$$u(x_k, x_i) \quad \text{– covariance.}$$

When the input variables have no relationship to each other except for their functional relationship that defines the measurement model, then covariance between every pair of different input quantities is assumed to be *zero*. The results of uncertainty estimation according to the Gauss Formula include an estimate of the true value of the output quantity and an evaluation of the associated standard uncertainty. Furthermore, the sensitivity coefficients and percentage contributions that the different input quantities make to the squared standard uncertainty of the output quantity are computed.

The Monte Carlo results contain summary statistics for a sample that was drawn from the probability distribution of the output, such as mean standard deviation, median etc. Coverage intervals are determined for coverage probabilities of 99%, 95%, 90%, and 68%. The probability density of the output quantity is estimated for both method.

In the following subsections, the determination of the standard uncertainty of individual components of equation (4) is presented.

### 3.1.1. Evaluation of uncertainty of $R_i$

During the calibration and preparation of the device for measurements, the element properties (element value or its characteristics) were first determined in each of the measurement channels based on a single resistive standard element and based on the accuracy properties of the DAQ card.

First of all, the values of the resistors  $R_i$  (Fig. 2) in each of the channels were determined. The resistance of the reference resistor  $R_{ref}$  is  $5001 \Omega$  and its accuracy class index is  $0.05 \%$ , which corresponds to the expanded uncertainty equal to  $2.8 \Omega$  at a confidence level of approx.  $95 \%$  [Masnicki and Swisulski 2023].

The value of auxiliary resistance  $R_i$  can be calculated using the following formula:

$$R_i = R_{ref} \frac{U_s - U_i}{U_i} \quad (8)$$

The measured values of  $U_s$  and  $U_i$  for measured in a series of 30 elements for channel 1, and their standard deviations, are shown in Table 1.

**Table 1.** The voltages obtained during determination of  $R_i$

Input variables	Mean	Standard deviation
$U_s$ [V]	4.98207	0.00009
$U_i$ [V]	2.48859	0.00049

Source: own study.

By implementing the Gauss Formula software [NIST Uncertainty Machine 2023] and taking into account the measurement uncertainty of the DAQ card, a mean value of  $R_i$  and standard uncertainty equal to  $5010.83 \Omega$  and  $3.39 \Omega$  respectively are obtained.

### 3.1.2. Evaluation of uncertainty of $R_{Ti}$

Similarly, the values of thermistor resistances at specific temperatures  $0^\circ\text{C}$  and  $99.3^\circ\text{C}$  can be determined using the equation:

$$R_{Ti} = R_i \frac{U_{Ti}}{U_s - U_{Ti}} \quad (9)$$

The mean value of  $R_i$  was evaluated in Subsection 3.1.1. The appropriate parameters for voltages  $U_s$  and  $U_{Ti}$  are shown in Table 2.

**Table 2.** The voltages measured to determine the resistance of the thermistor at specific temperatures

Input variables	$T_i$ [ $^\circ\text{C}$ ]			
	0		99.3	
	Mean	Standard deviation	Mean	Standard deviation
$U_s$ [V]	4.97149	0.00007	4.90314	0.00010
$U_{Ti}$ [V]	4.20782	0.00008	0.82266	0.00036





Source: own study.

The mean values of  $R_{T_i}$  and corresponding standard uncertainties for specific temperatures were calculated using Gauss Formula software [NIST Uncertainty Machine 2023]. As in the previous case, the measurement uncertainty of type B was also considered. The mean value and standard uncertainty of the thermistor resistance are equal to 27609.7  $\Omega$  and 19.2  $\Omega$  at a temperature of 0°C and 1010.23  $\Omega$  and 0.867  $\Omega$  in temperature of 99.3°C respectively.

### 3.1.3. Evaluation of uncertainty of $\beta$

The material coefficient  $\beta$  of the thermistor and its uncertainty can be evaluated on the basis of the  $R_{T_i}$  values obtained for temperatures of 0°C ( $T_1$ ) and 99.3°C ( $T_3$ ) set with accuracy of 0.1°C using the following formula:

$$\beta = \ln\left(\frac{R_{T_3}}{R_{T_1}}\right) \frac{1}{\left(\frac{1}{T_3} - \frac{1}{T_1}\right)} \quad (10)$$

The mean values of  $R_{T_1}$  and  $R_{T_3}$ , and their uncertainties are determined in Subsection 3.1.2.

The mean value of  $\beta$  and standard uncertainty are equal to 3389.1 K and 1.13 K respectively.

### 3.1.4. Evaluation of the uncertainty of the temperature measurement channel

The combined measurement uncertainty (7), relating to the temperature measurement channel modelled by equation (4), is calculated using the two different methods mentioned previously. Both correlated and uncorrelated variables were considered. Tables 3 and 4 show the results for the temperature measurement channel selected but are valid for all other channels. In the Monte Carlo method, the number of realisations of the output quantity was assumed to be 1 000 000, and the random number generator seed was set to 71.

The values of voltages  $U_s$  and  $U_i$  (Table 3) were obtained at the DAQ output in the developed instrument during verification measurements for the reference temperature of 49.7°C (322.85 K). In calculations using the Gauss Formula, the determined temperature was 323.115 K (49.965°C), and the combined measurement uncertainty was 0.145 K and 0.13 K for correlated and uncorrelated variables respectively.

Table 3 contains the sensitivity coefficients as defined in (7) and the percentage contributions that the different input quantities make to the squared standard uncertainty of the output quantity.

**Table 3.** The Gauss Formula results

Input variables	Mean values of input variables	Standard deviation of input variables	Sensitivity coefficients		Percentage contribution [%]	
			uncorrelated variables	correlated variables	uncorrelated variables	correlated variables
$U_s$	4.93092 V	0.00007 V	11	11	0.003	0.3200
$U_i$	2.20501 V	0.00029 V	-25	-25	0.260	0.0037
$\beta$	3389.1 K	1.13 K	-17e-03	-17e-03	1.900	2.3000
$R_{T_0}$	27609.7 $\Omega$	19.2 $\Omega$	1.1e-03	1.1e-03	2.200	2.7000
$R_i$	5010.83 $\Omega$	3.39 $\Omega$	-6.1e-03	-6.1e-03	2.100	2.6000
$T_0$	273.15 K	0.1 K	1.4	1.4	94.000	120.0000
Correlation	-	-	-	-	-	- 23.0000

Source: own study.

If the input quantities are uncorrelated, then these contributions amount to approximately 100%. If they are correlated, then the contributions may amount to more or less than 100%, depending on the absolute values and signs of the correlations. Sensitivity coefficients provide a measure of how sensitive the output quantity  $T$  (4) is to a change in given input quantity.

Note that this effect is most noticeable at voltage  $U_s$  and  $U_i$ , and temperature  $T_0$ , whether the input quantities are correlated or not (Tab. 3). The accuracy of determining the  $T_0$  parameter has the greatest impact on the accuracy of temperature calculation according to (4).

The same results were also obtained with regard to the temperature values and the combined measurement uncertainty determined using the Monte Carlo method (Tab. 4). It shows the designated uncertainty intervals for various coverage factors, for both correlated and uncorrelated variables.

**Table 4.** The Monte Carlo Method results for temperature channel accuracy evaluation

Summary statistics	Uncorrelated variables	Correlated variables
Average [K]	323.115	323.115
Standard deviation [K]	0.145	0.13
Median [K]	323.115	323.115

MAD* [K]	0.14				0.13			
Coverage probability [%]	99	95	90	68	99	95	90	68
Coverage interval [K]	322.74 - - 323.49	322.83 - - 323.40	322.88 - - 323.35	322.97 - - 323.26	322.78 - - 323.45	322.86 - - 323.37	322.90 - - 323.33	322.99 - - 323.25
Coverage factor	2.6	2	1.6	1	2.6	2	1.7	1

\*MAD denotes the median absolute deviation from the median, multiplied by a factor (1.4826) that makes the result comparable to the standard deviation when applied to samples from Gaussian distributions.

Source: own study.

In Figure 3, the calculated probability density function is presented.

Comparing the estimated probability density of the output quantity (solid blue line) and the probability density (dotted red line) of the Gaussian distribution (with the same mean and standard deviation as the output quantity), it can be seen that the Gaussian approximation is very accurate in this case.

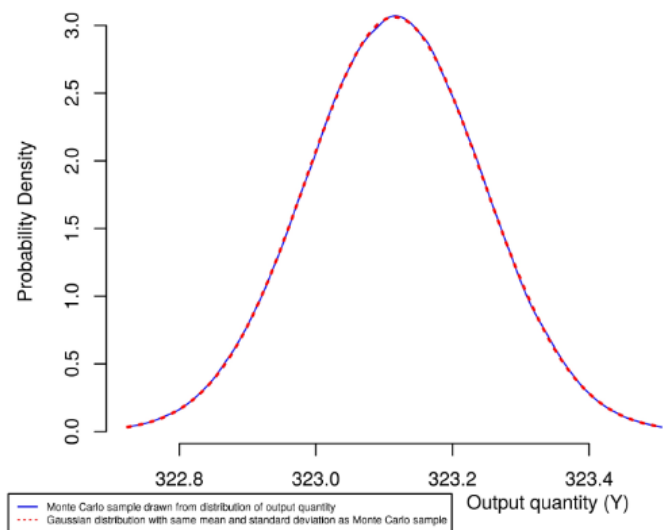


Fig. 3. The probability density of output quantity

Source: own study.

### 3.2. Empirical evaluation of uncertainty

After calibrating the instrument, verification measurements were made. During the tests, the temperatures of all channels were compared with the  $T_{ref}$  reference temperatures, measured with the DT-35 digital thermometer [Thermometer DT-34 2023].

Table 5 shows sample verification measurements on Channel 1, which is representative of all other channels, and the deviation from the digital thermometer reference temperature.

**Table 5.** The measurement results of  $T_i$  temperatures (channel1) in relation to the reference temperatures  $T_{ref}$

$T_{ref}$ [°C]	23.30	29.10	40.10	50.6	59.80	69.80	79.10	88.40	100.20
$T_i$ [°C]	23.35	29.10	40.12	50.64	59.86	69.82	79.24	88.57	100.54

Source: own study.

The largest empirically obtained deviation in this channel from reference temperature does not exceed 0.35 °C. There were no major deviations in any of the other channels. The graphical presentation of deviation in all 10 channels is shown in Figure 4.

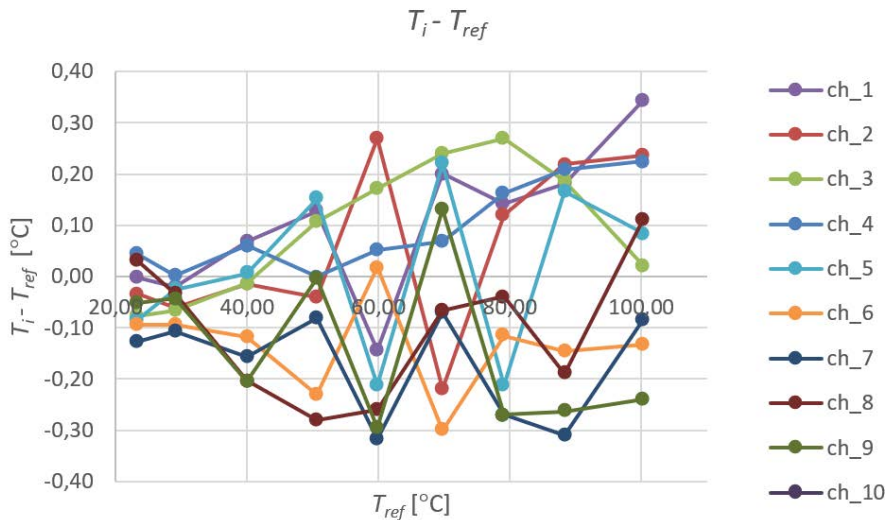


**Fig. 4.** The course of differences between the temperatures determined in ten channels and the reference temperatures in relation to the reference temperatures ( $T_{ref}$ )

Source: [Masnicki and Swisulski 2023].

In addition, the average temperatures  $T_A$  (Tab. 6), calculated from the temperatures obtained in all 10 channels, were compared with the indication of a digital thermometer.

**Table 6.** The measurement results for  $T_A$  temperatures averaged from 10 sensors in relation to the reference temperatures  $T_{ref}$

$T_{ref}$ [°C]	23.30	29.10	40.10	50.6	59.80	69.80	79.10	88.40	100.20
$T_A$ [°C]	23.27	29.04	39.99	50.57	59.73	69.75	79.00	88.40	100.30

Source: own study.

The greatest deviation between the average temperatures measured in 10 channels and the reference thermometer does not exceed 0.1°C.

#### 4. CONCLUSIONS

In the measurement system, circuits used to identify the characteristics of thermistors and auxiliary resistors in voltage dividers were used as measurement channels. In the process of measurement, the values of elements and coefficients determined while identifying the characteristics of individual measurement channels of the device developed were used. The procedures for identifying the characteristics of measurement channels and their calibration were carried out together with the process of defining standard deviations of measurement series of voltage samples on the output of the ADC – the final hardware circuit of each measurement channel. The high resolution of the DAQ card was accompanied by measurement errors of 2  $\mu$ V, which does not have a major impact on the overall accuracy in the measurement channel. One major source of measurement errors was elements and signals in the hardware part of the measurement channel. A further part of the measurement channel consists of software-related procedures. Because of floating point arithmetic being used in the program algorithms of each channel, the assumption of a negligible impact of errors in software procedures on the overall accuracy of temperature measurement is justified.

The basis for a theoretical assessment of the temperature measurement accuracy is the mathematical model of the hardware part of the measurement channel, which shows the stages in the processing of measurement information from the temperature sensor to the output of the ADC converter by means of a mathematical relationship. The transformation of this equation into a form that enables the temperature to be determined also enables, on the basis of the values of other factors of the equation, a theoretical assessment of the accuracy of the measured temperature.

An empirical assessment of the accuracy of measurement results was made in instrument verification procedures by comparing the measured temperature value determined in the measuring channel of the device with the same temperature measured with a reference digital thermometer. The conducted experiments confirmed the satisfactory operation of the designed multi-channel temperature measurement system and acceptable accuracy of temperature measurement channels.

Full compliance of the results and conclusions with the research objective was achieved. Both the results obtained using two methods of theoretical accuracy assessment in the measuring channels of the developed device and the empirical method of verifying the accuracy of temperature measurements confirmed the correctness of the adopted concept of the instrument and its good metrological properties.

## REFERENCES

- JCGM 100: *Evaluation of Measurement Data — Guide to the Expression of Uncertainty in Measurement*, 2008, [https://www.bipm.org/documents/20126/2071204/JCGM\\_100\\_2008\\_E.pdf/cb0ef43f-baa5-11cf-3f85-4dcd86f77bd6?elqTrackId=2AF2E4569E5788A3689CDE7ED7E569DF&elqaid=1568&elqat=2](https://www.bipm.org/documents/20126/2071204/JCGM_100_2008_E.pdf/cb0ef43f-baa5-11cf-3f85-4dcd86f77bd6?elqTrackId=2AF2E4569E5788A3689CDE7ED7E569DF&elqaid=1568&elqat=2) (14 May 2023).
- JCGM 101: *Evaluation of Measurement Data – Supplement 1 to GUM. Propagation of Distributions Using a Monte Carlo Method*, 2008, [https://www.bipm.org/documents/20126/2071204/JCGM\\_101\\_2008\\_E.pdf](https://www.bipm.org/documents/20126/2071204/JCGM_101_2008_E.pdf) (14 May 2023).
- JCGM 102: *Evaluation of Measurement Data – Supplement 2 to the GUM. Extension to Any Number of Output Quantities*, 2011, [https://www.bipm.org/documents/20126/2071204/JCGM\\_102\\_2011\\_E.pdf/6a3281aa-1397-d703-d7a1-a8d58c9bf2a5?version=1.6&t=1641293321173&download=true](https://www.bipm.org/documents/20126/2071204/JCGM_102_2011_E.pdf/6a3281aa-1397-d703-d7a1-a8d58c9bf2a5?version=1.6&t=1641293321173&download=true) (Accessed: 14 May 2023).
- Liu, K.Q., Pan, X.T., Cai, J.W., 2012, *Analysis of Multi-Channel Virtual Temperature Measurement System Hardware Design and Its Uncertainty*, *Applied Mechanics and Materials*, vol. 220–223, pp. 1423–1426.
- Masnicki, R., Mindykowski, J., Palczynska, B., 2022, *Experiment-Based Study of Heat Dissipation from the Power Cable in a Casing Pipe*, *Energies*, vol. 15(13).
- Masnicki, R., Swisulski, D., 2023, *Multi-Channel Virtual Instrument for Measuring Temperature – A Case Study*, *Electronics*, vol. 12(10).
- NI PXIe-6341, 2023, *Specifications*, <https://www.ni.com/docs/en-US/> (14 May 2023).
- NI PXIe-1082, 2023, *Specifications*, <https://www.ni.com/docs/en-US/bundle/pxie-1082-specs/page/specs.html#> (14 May 2023).
- NI PXIe-8135, 2023, *User Manual. National Instruments*, <https://www.ni.com/docs/en-US/bundle/pxie-8135rt-specs/page/specs.html> (14 May 2023).
- NIST *Uncertainty Machine*, 2023, <https://uncertainty.nist.gov/> (14 May 2023).
- NTC *Thermistor Accuracy Temperature Sensor Thermistor NTC 10K 1% 3950 Waterproof Probe*, 2017, OKYSTAR, <https://www.okystar.com/product-item/ntc-thermistor-ntc-10k-oky3065-5/> (14 May 2023).

- Pawłowski, E., Szlachta, A., Otomański, P., 2023, *The Influence of Noise Level on the Value of Uncertainty in a Measurement System Containing an Analog-to-Digital Converter*, *Energies*, vol. 16(3).
- Samoilenko, O., 2021, *The Calibration and Uncertainty Evaluation by Elementary Measurement Models*, *Measurements infrastructure*, vol. 1, pp. 1–10.
- Sârbu, G.C., 2018, *Evaluation of the Measurement Uncertainty in Thermoresistances Calibration*, *International Conference and Exposition on Electrical and Power Engineering (EPE)* [Preprint].
- SCB-68 and SCB-68A, 2023, *DAQ Multifunction I/O Accessory Guide*, <https://www.ni.com/en-us/support/documentation/supplemental/17/scb-68-and-scb-68a---daq-multifunction-i-o-accessory-guide.html> (14 May 2023).
- Steinhart, J.S., Hart, S.R., 1968, *Calibration Curves for Thermistors*, *Deep Sea Research and Oceanographic Abstracts*, vol. 15(4), pp. 497–503.
- Thermometer DT-34*, 2023, *High Accuracy Resistance Food Industrial Min Max Probe Digital Thermometer DT-34. Display Temperature Meter with 0.1°C Accuracy for Agriculture, Labs and Food. (-100°C to 270°C)*, <https://termoprodukt.co.uk/industrial-thermometer-dt-34> (14 May 2023).